PCCP

PAPER

View Article Online
View Journal | View Issue

Open Access Article. Published on 13 October 2022. Downloaded on 11/19/2024 11:00:08 PM.
This article is licensed under a Creative Commons Attribution 3.0 Unported Licence.

Check for updates

Cite this: *Phys. Chem. Chem. Phys.*, 2022, **24**, 25822

Reduced nucleophilicity: an intrinsic property of the Lewis base atom interacting with H in hydrogen-bonds with Lewis acids HX (X = F, Cl, Br, I, CN, CCH, CP)†

Ibon Alkorta [a] and Anthony Legon [b]

Received 29th August 2022,
Accepted 13th October 2022

DOI: 10.1039/d2cp03999k

rsc.li/pccp

Equilibrium hydrogen-bond dissociation energies D_e for the process B···HX = B + HX are calculated at the CCSD(T)(F12c)/cc-pVDZ-F12 level for ∼190 complexes B···HX. As established earlier, D_e values for such complexes can be described by the equation $D_e = cN_BE_A$, in which N_B and E_{HX} are the nucleophilicity and electrophilicity of the Lewis base B and the Lewis acid HX, respectively, and the constant c = 1 kJ mol^{-1}. Graphs of D_e as the ordinate and E_{HX} as the abscissa are presented for 26 series of hydrogen-bonded complexes B···HX. The Lewis base is fixed and HX is HF, HCl, HBr, HI, HCN, HCCH and HCP in each series. Each plot yields a good straight line, the slope of which is the nucleophilicity N_B of B. The Lewis bases are chosen for their simplicity and all have at least one non-bonding electron pair carried by the atom directly involved in the B···HX hydrogen bond. The direction of the minimum value σ_{min} of the molecular electrostatic surface potential on the 0.001 e bohr^{-3} iso-surface in the chosen bases B usually coincides with the axis of a non-bonding electron pair. The gradient of a graph of D_e/σ_{min} plotted against E_{HX} defines a reduced nucleophilicity $И_B = N_B/\sigma_{min}$ in the sense that $И_B$ appears to be a property only of the atom of B that is directly involved in the B···HX hydrogen bond, independent of the remainder of B. For example, the values of the reduced nucleophilicity for the series of isocyanide complexes CH_3NC···HX, HNC···HX and FNC···HX are 0.0343(16), 0.0337(18) and 0.0332(18), respectively, while those for the corresponding series of cyanide complexes are 0.0337(23), 0.0329(24) and 0.0333(23).

1. Introduction

There have been many proposals to describe non-covalent interactions (particularly in respect of hydrogen bonding) in terms of various observable properties of the component molecules in complexes. For example, Drago and co-workers proposed a relationship between the dissociation enthalpy of hydrogen-bonded complexes and two parameters associated with the two components, one assigned to the hydrogen-bond donor and the other assigned to the hydrogen-bond acceptor.[1,2] Taft and Abraham described hydrogen-bond complexation in terms of acidity α and basicity β scales of the hydrogen-bond donor and acceptor molecules, respectively,[3–7] while Platts predicted α and β[8–11] by means of theory. Both Steiner[12–14] and Limbach[15,16] discussed hydrogen bonding of complexes Y···HX investigated by NMR spectroscopy in terms of the distances r(X–H) and r(H···Y), with subsequent theoretical interpretation by Alkorta and Elguero.[17,18] Relationships between electron density properties and intermolecular distances were pursued by Espinosa[19] and others.[20]

In this article we introduce the concept of a quantitative, reduced nucleophilicity associated with an isolated Lewis base B. The terms nucleophile and electrophile were first defined[21] in 1933 and since then there has developed an extensive literature concerned with scales of nucleophilicity and electrophilicity, most of which are based on rates of reaction. See for example the review by Mayr and Patz.[22] The subject is not without controversy.[23] In 1987, an alternative definition of these quantities in terms of weak interactions between molecules was proposed, namely in terms of the intermolecular stretching force constant k_σ of isolated hydrogen-bonded complexes B···HX formed between a Lewis base B and a Lewis acid HX. The definition was expressed by means of eqn (1):

$$k_\sigma = c' N_B E_{HX}, \quad (1)$$

[a] Instituto de Química Médica (IQM-CSIC), Juan de la Cierva, 3, E-28006 Madrid, Spain. E-mail: ibon@iqm.csic.es; Tel: +34 915622900
[b] School of Chemistry, University of Bristol, Cantock's Close, Bristol BS8 1TS, UK. E-mail: a.c.legon@bristol.ac.uk; Tel: +44 (0)117 331 7708

† Electronic supplementary information (ESI) available. See DOI: https://doi.org/10.1039/d2cp03999k

 This journal is © the Owner Societies 2022

Open Access Article. Published on 13 October 2022. Downloaded on 11/19/2024 11:00:08 PM. This article is licensed under a Creative Commons Attribution 3.0 Unported Licence.

in which N_B is the nucleophilicity of B, E_{HX} is the electrophilicity of HX and c' is a constant.[24] Later, it was shown that k_σ is directly proportional to the equilibrium dissociation energy D_e for the process B···HX = B + HX for a wide range of hydrogen-bonded and halogen-bonded complexes,[25] thus allowing eqn (1) to be rewritten as:

$$D_e = cN_BE_{HX}. \quad (2)$$

It is convenient to choose $c = 1$ kJ mol^{-1}, so that N_B and E_{HX} are dimensionless when D_e is expressed in units of kJ mol^{-1}. For a series B···HX in which the Lewis acid HX is held constant and B is varied, it then follows from eqn (2) that the graph having D_e as the ordinate and N_B as the abscissa is a straight line through the origin and having a gradient E_{HX}. Eqn (2) has been successfully tested recently for a wide range of hydrogen- and halogen-bonded complexes B···HX and B···XY (X and Y are halogen atoms), as well as for complexes involving other types of non-covalent interaction.[26–29] By means of a least-squares fit of the D_e values of 250 hydrogen-bonded, halogen-bonded and other types of complex, a set of N_B and E_{HX} values for 23 and 11 simple Lewis acids and bases, respectively, has been established.[27]

It is generally accepted that for hydrogen- and halogen-bonded complexes the intermolecular interaction has a large electrostatic contribution and geometries of complexes can be modelled on this basis.[30] A popular method of describing the electrostatic charge distribution associated with a molecule is the so-called molecular electrostatic surface potential (MESP), which is the potential energy of a unit positive charge at a surface of constant electron density, with the iso-surface at which the charge density is 0.001 e bohr^{-3} in common usage.[31] Examination of the MESP of Lewis acids such as HCl reveals that the value on the molecular axis near to H is the maximum (positive) potential σ_{max} for the defined surface and is therefore the most electrophilic region of the molecule. In a recent article,[32] we showed the quantity D_e/σ_{max} is an intrinsic property of, for example, the H atom of a series of hydrogen halides HX and is independent of the atom X. Dividing eqn (2) by σ_{max} gives

$$D_e/\sigma_{max} = cN_B(E_{HX}/\sigma_{max}) = N_B\Xi_{HX}, \quad (3)$$

where $\Xi_{HX} = (E_{HX}/\sigma_{max})$. As was shown in detail in ref. 32, plots of D_e/σ_{max} *versus* N_B in which B varies but HX is held constant lead to straight line graphs of gradient $\Xi_A = E_A/\sigma_{max}$ which is dimensionless if $c = 1.0$ kJ mol^{-1} and D_e and σ_{max} are in kJ mol^{-1}. Given that eqn (2) and (3) are conformal and given the conclusion of ref. 32 that Ξ_{HX} is an intrinsic property of H, independent of the atom or group X attached to it, it is reasonable to describe Ξ_{HX} as the reduced electrophilicity of the acid HX. The importance of dimensionless and reduced quantities in physics and chemistry has been reviewed in a recent book.[33]

In this article, we examine whether there is an analogous reduced nucleophilicity defined as $И_B = N_B/\sigma_{min}$. For linear and symmetric-top molecules, such as HCN and CH_3CN, that carry an axial non-bonding electron pair, it is often the case that the MESP near the terminal atom is the minimum value σ_{min} on the chosen iso-surface and is therefore the most nucleophilic region of the molecule. Dividing eqn (2) by σ_{min} leads to

$$D_e/\sigma_{min} = c(N_B/\sigma_{min})E_{HX} = cИ_BE_{HX} \quad (4)$$

A question of interest resulting from eqn (4) is: if D_e/σ_{min} were plotted against E_{HX} for a series of complexes B···HX in which X varies but B is unchanged, is it reasonable to refer to the gradient of the resulting straight line as the reduced nucleophilicity $И_B$ of the base B, and to ask whether this quantity is an intrinsic property of the atom of the Lewis base B interacting with H in the B···HX hydrogen bond, that is whether $И_B$ is independent of the remainder of B? This article will seek answers to this question by examining a wide range of Lewis bases involved in the hydrogen-bonded complexes B···HX (X = F, Cl, Br, I, CN, CP and CCH).

2. Theoretical methods

The geometries of the isolated monomers and complexes were optimized at the CCSD(T) (F12c) computational level[34,35] with the cc-pVDZ-F12 basis set[36] using the frozen-core approximation. The Cartesian coordinates of the optimized geometries are available in Table S1 of the ESI.† The equilibrium dissociation energies D_e were calculated as the difference between the electronic energy of the complex and the sum of those of the isolated monomers (see Table S2 of the ESI†), with correction for basis set superposition error (BSSE) using the full counterpoise method of Boys and Bernadi.[37] These calculations were conducted with the MOLPRO program.[38] The molecular electrostatic surface potentials (MESP) of the isolated Lewis bases were calculated at the MP2/aug-cc-pVTZ wavefunction with the GAUSSIAN program[39] and analyzed on the 0.001 e bohr^{-3} electron density iso-surface with the Multiwfn program.[40] Some MESPs used for illustrative purposes in various figures were calculated at the M06-2X/aug-cc-pVDZ level with the SPARTAN program.[41]

3. Results

3.1 Series of linear complexes B···HX in which the hydrogen-bond is to a terminal C atom, B = SC, SeC, OC

Fig. 1(a) shows a plot of D_e *versus* E_{HX} for the three series of hydrogen-bond complexes OC···HX, SC···HX and SeC···HX, where X = F, Cl, Br, I, CN, CCH and CP. The values of the electrophilicities E_{HX} are set out in Table 1 for convenience and are from ref. 27, except for E_{HBr} and E_{HI} which are reported in ref. 42. Note that eqn (2) (with $c = 1$ kJ mol^{-1}) is obeyed in good approximation by all three series, that the gradients for the Lewis bases = SC and SeC are identical but that for OC is smaller by a factor of two. Fig. 1(b) shows plots of D_e/σ_{min} *versus* E_{HX} for the same three series. σ_{min} is in each case the value of the MESP on the 0.001 e bohr^{-3} electron density iso-surface on the axis of the diatomic molecule and near to C. Values of σ_{min} used in this article were calculated at the MP2/aug-cc-pVTZ

Open Access Article. Published on 13 October 2022. Downloaded on 11/19/2024 11:00:08 PM.
This article is licensed under a Creative Commons Attribution 3.0 Unported Licence.

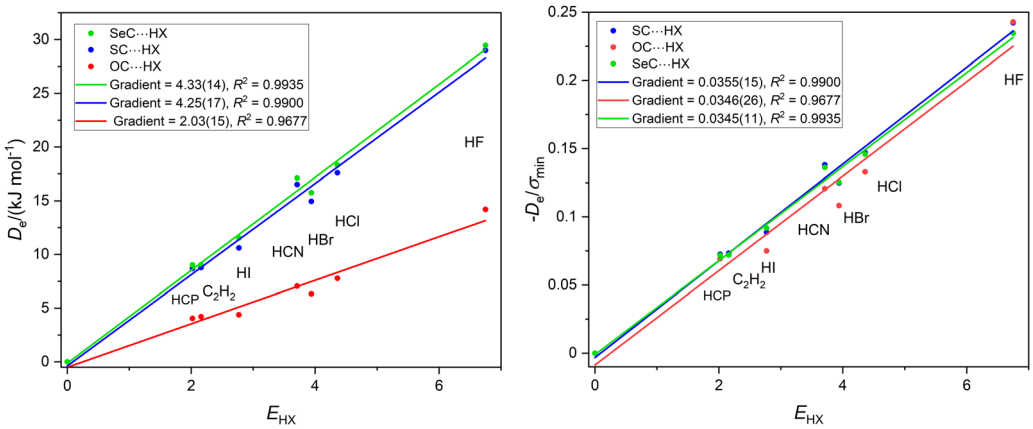

Fig. 1 (a) A plot of D_e *versus* E_{HX} for the series OC···HX, SC···HX and SeC···HX for X = F, Cl, Br, I, C≡N. C≡CH and C≡P. (b) A plot of D_e/σ_{min} for the same series.

Table 1 Electrophilicities[a] E_{HX} of the Lewis acids HX (X = F, Cl, Br, I, CN, CCH, CP)

Lewis acid HX	Electrophilicity E_{HX}
HF	6.75
HCl	4.36
HBr	3.94
HI	2.77
HCN	3.71
HCCH	2.16
HCP	2.02

[a] Values are from ref. 27, except for those of HBr and HI, which are from ref. 42.

Table 2 Minimum values (σ_{min}) of the molecular electrostatic surface potentials (MESP)[a] of 32 Lewis bases calculated at the MP2/aug-cc-pVTZ level of theory

Lewis base	H-Bond to atom[b]	σ_{min}/kJ mol^{-1}	Lewis base	H-Bond to atom[b]	σ_{min}/kJ mol^{-1}
O≡C	Carbon	−58.5	H_2O	Oxygen	−135.1
S≡C	Carbon	−119.7	$H_2C{=}O$	Oxygen	−121.4
Se≡C	Carbon	−125.6	$H_2C{=}C{=}O$	Oxygen	−64.5
$CH_3N{\equiv}C$	Carbon	−161.8	$(CH_3)_2O$	Oxygen	−130.2
HN≡C	Carbon	−138.9	Oxirene	Oxygen	−135.8
FN≡C	Carbon	−106.9	H_2S	Sulfur	−69.3
$CH_3C{\equiv}N$	Nitrogen	−159.2	$H_2C{=}S$	Sulfur	−74.7
HC≡N	Nitrogen	−133.7	$(CH_3)_2S$	Sulfur	−95.1
FC≡N	Nitrogen	−119.1	Thiirene	Sulfur	−100.6
N≡N	Nitrogen	−35.8	S=S	Sulfur	−50.3
P≡N	Nitrogen	−131.5	H_3N	Nitrogen	−155.9
O=C=O	Oxygen	−44.6	$(CH_3)_3N$	Nitrogen	−133.2
S=C=O	Oxygen	−46.2	Aza-tetrahedrane	Nitrogen	−140.2
H–B	Boron	−134.5	Cl_3N	Nitrogen	−49.5
H_3C–B	Boron	−160.3	H_3P	Phosphorus	−67.4
F–B	Boron	−89.3	$(CH_3)_3P$	Phosphorus	−114.4

[a] The MESP is the potential energy of a unit positive charge (proton) at the iso-surface for which the electron density is 0.001 e bohr^{-3}. The minimum (*i.e.* most negative) value of the MESP coincides in all but one case with the direction of the axis of a non-bonding electron pair carried by the H-bond acceptor atom of the Lewis base. NCl_3 is an exception in that the MESP along a Cl non-bonding pair direction is actually the minimum value. [b] Atom involved in the hydrogen bond with the Lewis acid HX (see text).

level of theory and are listed in Table 2. The gradients of the 3 straight lines in Fig. 1(b) are identical within the fitting error, with the mean value 0.0349(4). According to eqn (4), the gradient of such lines is the reduced nucleophilicity $И_B$ of the non-bonding electron pair associated with C in the three molecules SC, SeC and OC.

3.2 Series of linear or symmetric-top complexes B···HX in which the hydrogen-bond is to a terminal C atom. B = CH_3NC, HNC and FNC

The three series CH_3NC···HX, HNC···HX and FNC···HX (X = Cl, Br, I, CN, CCH and CP) are of interest here for two reasons. First, the hydrogen bond from HX is again to an axial, terminal carbon atom in these linear or symmetric-top molecules and secondly relative to H of HNC the CH_3 and F groups attached to the isocyanide group are electron donating and electron withdrawing, respectively. The plots of D_e and D_e/σ_{min} *versus* E_{HX} are in Fig. 2(a) and (b), respectively. The values of σ_{min} are available in Table 2.

We note from Fig. 2(a) that the gradients are in the order CH_3NC···HX > HNC···HX > FNC···HX. Eqn (2) indicates that a plot of D_e *versus* E_{HX} should be a straight line through the origin with gradient N_B, the nucleophilicity of the Lewis base involved. Thus, the order of the nucleophilicities of the isocyanides is N_{CH_3NC} = 5.55(25) > N_{HNC} = 4.68(24) > N_{FNC} = 3.55(20). This is the order expected from the inductive effects of the groups R in RNC, that is CH_3 pushes electron density towards the non-bonding electron pair of the terminal C atom relative to H, while F is electron-withdrawing relative to H.

Fig. 2(b) shows that division of D_e by σ_{min} reduces the three straight lines of Fig. 2(a) to a single line, for the gradients are now identical within the fitting error. Hence, it seems reasonable, according to eqn (4), to refer to the mean gradient = 0.0337(5) as

Open Access Article. Published on 13 October 2022. Downloaded on 11/19/2024 11:00:08 PM.
This article is licensed under a Creative Commons Attribution 3.0 Unported Licence.

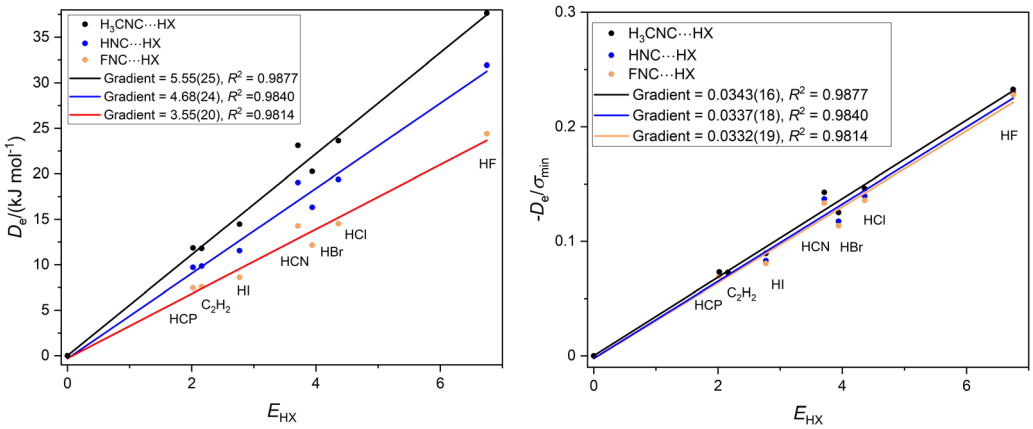

(a) (b)

Fig. 2 (a) A plot of D_e *versus* E_{HX} for the series $CH_3NC\cdots HX$, $HNC\cdots HX$ and $FNC\cdots HX$ where X = F, Cl, Br, I, C≡N. C≡CH and HC≡P. (b) A plot of D_e/σ_{min} for the same three series.

the reduced nucleophilicity $И_{RNC}$. This appears to be an intrinsic property of isocyanide group, independent of the atom or group that is attached to it. Moreover, this value of $И_{RNB}$ is very close to that deduced for the series SC, SeC and OC in Section 3.1. It appears that $И_C$ could even be an intrinsic property of the terminal C atom in a linear, hydrogen-bonded complex, independent of the atoms/groups attached to that C atom. Alternatively, the close agreement of the two values of $И_B$ might be just a coincidence.

3.3 Series of linear or symmetric-top complexes B···HX in which the hydrogen bond is to a terminal N atom. B = CH_3CN, HCN or FCN, (X = F, Cl, Br, I, CN, CCH, CP) and B = PN and N_2

It is of interest to examine the series of hydrogen-bonded complexes RCN···HX (X = F, Cl, Br, I, CN, CCH, CP) in which the hydrogen bond is to the terminal, axial nitrogen atom in the cyanides RCN (R = CH_3, H or F) and to compare the results with those discussed for the corresponding series RNC···HX involving isocyanides. Fig. 3(a) contains the graphs of D_e *versus* E_{HX} for the three series $CH_3CN\cdots HX$, $HCN\cdots HX$ and $FCN\cdots HX$, while Fig. 3(b) is the corresponding graph, but with D_e/σ_{min} as the ordinate.

The results in Fig. 3 are very similar to those for the corresponding RNC series in Fig. 2, except for a slightly larger scatter. The gradients in Fig. 3(a) are (according to eqn (2) when c is set to 1 kJ mol^{-1}) the nucleophilicities $N_{R\text{–}CN}$ of the three cyanides. The values are 5.37(37), 4.40(33) and 3.92(27) for R = CH_3CN, HCN and FCN, respectively, an order in agreement with the relative inductive effects of CH_3, H and F found for the R-NC series in Section 3.2. In Fig. 3(b), division of D_e by σ_{min} leads to a conflation of the three lines and again the gradients, which according to eqn (4) are the values of the reduced nucleophilicity $И_{RCN}$, are equal within the fitting error, with a mean value of 0.0333(6). Thus, the $И_{RCN}$ values are independent of the group R attached to the CN group and are (possibly by coincidence) identical within the fitting errors with the values found for the RNC series.

A question that arises is: is the reduced nucleophilicity $И_{RCN}$ an intrinsic property of the terminal N atom or does it depend

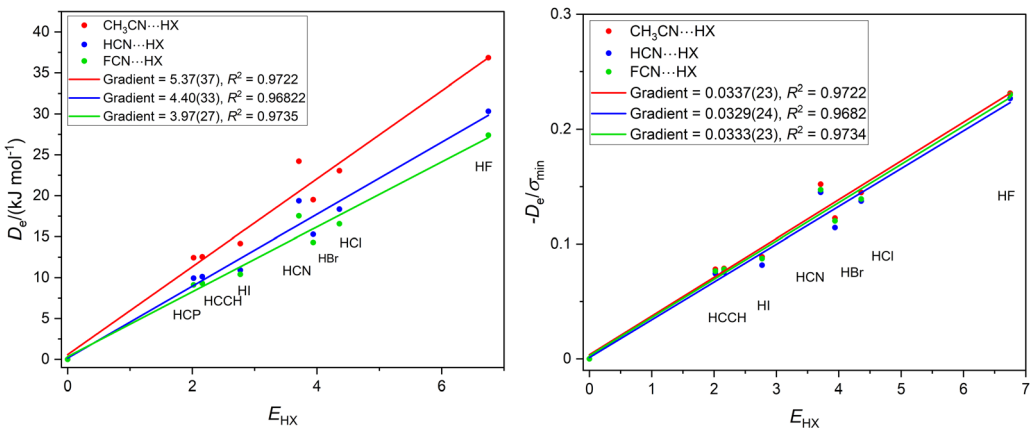

(a) (b)

Fig. 3 (a) A plot of D_e *versus* E_{HX} for the series $CH_3CN\cdots HX$, $HCN\cdots HX$ and $FCN\cdots HX$ where X = F, Cl, Br, I, C≡N. C≡CH and C≡P. (b) A plot of D_e/σ_{min} for the same three series.

Open Access Article. Published on 13 October 2022. Downloaded on 11/19/2024 11:00:08 PM.
This article is licensed under a Creative Commons Attribution 3.0 Unported Licence.

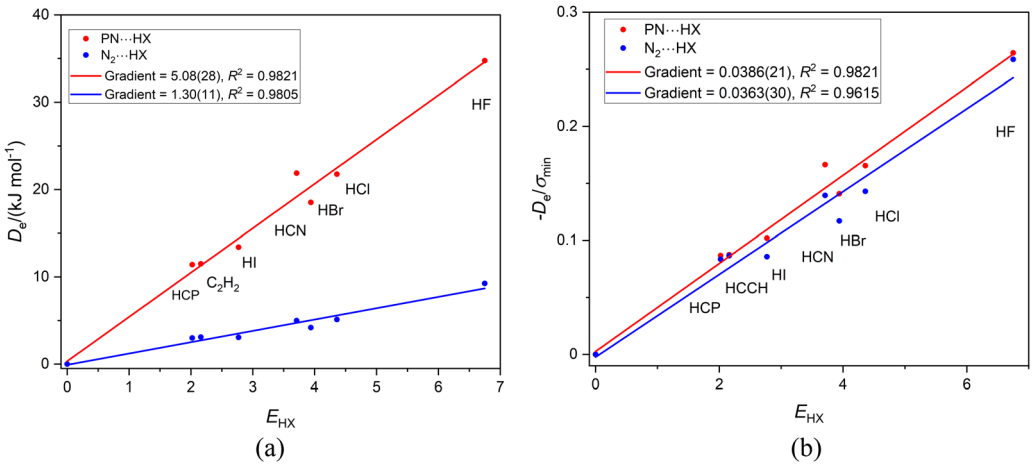

Fig. 4 (a) A plot of D_e *versus* E_{HX} for the series PN···HX and N_2···HX where X = F, Cl, Br, I, C≡N. C≡CH and C≡P. (b) A plot of D_e/σ_{min} for the same two series.

on the C atom of the CN group also? This can be tested by considering the two series of hydrogen-bonded complexes N_2···HX and PN···HX (X = F, Cl, Br, I, CN, CCH, CP) both of which are composed of linear complexes having a hydrogen bond to a nitrogen atom. Fig. 4(a) displays the D_e *versus* E_{HX} plot for both series, while Fig. 4(b) shows the result of diving D_e by σ_{min}. Fig. 4(b) reveals that, within (the fairly large) standard deviations of the two fits, the gradients are equal and therefore the $И_{PN}$ and $И_{N2}$ values are identical. These values are also similar (given the large errors) to the $И_{RCN}$.

3.4 Series of linear complexes B···HX in which the hydrogen bond is to a terminal O atom of a linear molecule. B = OCO and SCO, (X = F, Cl, Br, I, CN, CCH, CP).

Fig. 5(a) and (b) show the graphs of D_e *versus* E_{HX} and D_e/σ_{min} *versus* E_{HX}, respectively, for the linear complexes OCO···HX and SCO···HX having the order of the atoms indicated, that is having a hydrogen bond to a terminal oxygen atom. The gradients in Fig. 4(a) are almost equal, thereby indicating (according to eqn (2)) that the nucleophilicities of the O atoms in OCS and OCO are nearly equal. Division of D_e by σ_{min} again results in the precise coincidence of the points for the two sets of complexes. Moreover, the gradients (equal within the standard deviation of the fits) are the reduced nucleophilicities of carbon dioxide and carbonyl sulfide and have the values. $И_{oco}$ = 0.0372(36) and $И_{sco}$ = 0.0380(37).

All the evidence so far presented indicates that when the terminal atom of a linear or symmetric-top Lewis base molecule forms a hydrogen-bonded complex B···HX, where X = F, Cl, Br, I, CN, CCH or CP, the reduced nucleophilicity is independent of the nature of the terminal atom and the atoms in the base that are connected to it. Unfortunately, the errors in the individual values of the $И_{Lewis\ base}$ are quite significant.

3.5 Series of linear complexes B···HX in which the hydrogen bond is to a terminal boron atom in a Lewis base, R–B···HX, where R = CH_3, H and F (X = F, Cl, Br, I, CN, CCH, CP)

Recently,[42] we examined the effects of the group R on the dissociation energy D_e of the complexes R–B···HX, in which

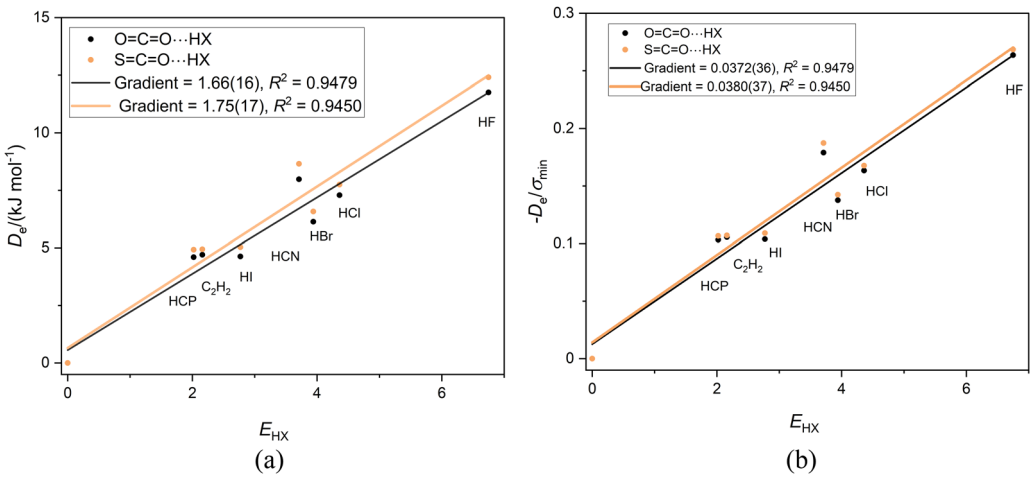

Fig. 5 (a) A plot of D_e *versus* E_{HX} for the series OCO···HX and SCO···HX for X = F, Cl, Br, I, C≡N. C≡CH and C≡P. (b) A plot of D_e/σ_{min} for the same two series.

Open Access Article. Published on 13 October 2022. Downloaded on 11/19/2024 11:00:08 PM.
This article is licensed under a Creative Commons Attribution 3.0 Unported Licence.

there is a hydrogen-bond to the axial non-bonding electron pair carried by the boron atom. The aim was define scales of nucleophilicity and the inductive effect that depend on the effect of R on hydrogen-bond interaction at boron rather than the more common definition in terms of rates of chemical reaction. Noting that fluoroborylene F–B is isoelectronic with OC and N_2 (Lewis bases involved in earlier sections), it is of interest to compare the three series F–B···HX, H–B···HX and CH_3B···HX. Fig. 6(a) displays the graph of D_e *versus* E_{HX} (X = F, Cl, Br, I, CN, CCH, CP) for these complexes involving the Lewis bases F–B, H–B and CH_3B. As discussed earlier, the gradient of each straight lines through the origin in Fig. 6(a) is, according to eqn (2) with c = 1.0 kJ mol^{-1}, the nucleophilicity of the Lewis base R–B. The values are N_{CH_3B} = 6.10(12), N_{HB} = 4.97(13) and N_{FB} = 3.16(12), which is consistent with chemical experience that CH_3 pushes electron density onto the B atom relative to H while F withdraws electron density.

Fig. 6(b) again shows, in accordance with eqn (4), with c chosen as 1.0 kJ mol^{-1}, that the reduced nucleophilicities of CH_3B, HB and FB are identical within the fitting error. Moreover, these values $И_{CH_3B}$, $И_{HB}$ and $И_{FB}$ appear to be identical with those examined in Sections 3.1–3.4, inclusive, although some of the errors generated in fitting the various straight lines are quite large. If this conclusion is valid, it implies that, for the types of simple Lewis bases examined so far, the quantity $И_{\text{Lewis base}}$ defined by the gradients of the D_e/σ_{min} *versus* E_{HX} plots for the series is an intrinsic property of the interaction of the base with the series of H-bond donors defined.

3.6 Non-linear complexes in which the hydrogen bond is to an oxygen or sulfur atom of an asymmetric-top molecule

In this article so far, the discussion has been restricted to either linear or symmetric top, hydrogen-bonded complexes B···HX in which the Lewis base B is a linear molecule or a symmetric-top molecule. Moreover, the symmetric-top molecules B carry an extended chain of atoms on the top axis so that the off-axis atoms are remote from HX. In these examples, the graphs of D_e/σ_{min} *versus* E_{HX} for different Lewis bases B, but having the same terminal atom acting as a hydrogen bond acceptor, fall on a single straight line (the gradient of which defines a reduced nucleophilicity of B). The question that arises is: can a reduced nucleophilicity be defined when B is an asymmetric-top molecule or a symmetric-top molecule in which the acceptor atom might lie closer to the off-axis atoms of the top?

We begin with complexes in which the oxygen atom in an asymmetric-top molecule is the hydrogen-bond acceptor atom. The Lewis bases chosen for this category are oxirene (oxacyclopropene), dimethyl ether $(CH_3)_2O$, formaldehyde $H_2C{=}O$, ketene $H_2C{=}C{=}O$ and water H_2O. Fig. 7(a) and (b) exhibit the D_e *versus* E_{HX} and D_e/σ_{min} *versus* E_{HX} graphs, respectively, for this series involving oxygen as the hydrogen-bond acceptor atom. Fig. 7(a) reveals that the graphs of D_e *versus* E_{HX} are again good straight lines when the origin is included as a point.

The complexes involved in Fig. 7 all have a plane of symmetry which includes the oxygen atom, as is clear for the example of oxirene···HCl drawn to scale in Fig. 8(a). The principal axis coordinates of the five types of complex B···HX (X = F, Cl, Br, I, CN, CCH and CP) discussed in Fig. 7 are available in the ESI† (Table S1). The HX molecule in oxirene-HX forms a hydrogen bond to one of the two non-bonding electron pairs carried by the oxygen atom. This is clear from the molecular electrostatic surface potential (MESP) of oxirene, which is shown in Fig. 8(b) and was calculated at the M06-2X/aug-cc-pVDZ level with the SPARTAN program.[41] The two deepest red regions of that surface are the most negative (and therefore most nucleophilic) areas and clearly are associated with the O atom non-bonding pairs. The half of the angle between the n-pair centres is about 60° and is in agreement with the angle 64.6° made by the H···O line with the oxirene C_2 axis. The geometry of $(CH_3)_2O$···HCl admits of a similar interpretation, while H_2O···HCl also has a pyramidal configuration[43] at O. $H_2C{=}O$···HCl and $H_2C{=}C{=}O$···HCl are planar with the angle C=O···H close to 120° consistent with a hydrogen bond to one of the O atom non-bonding electron pairs.

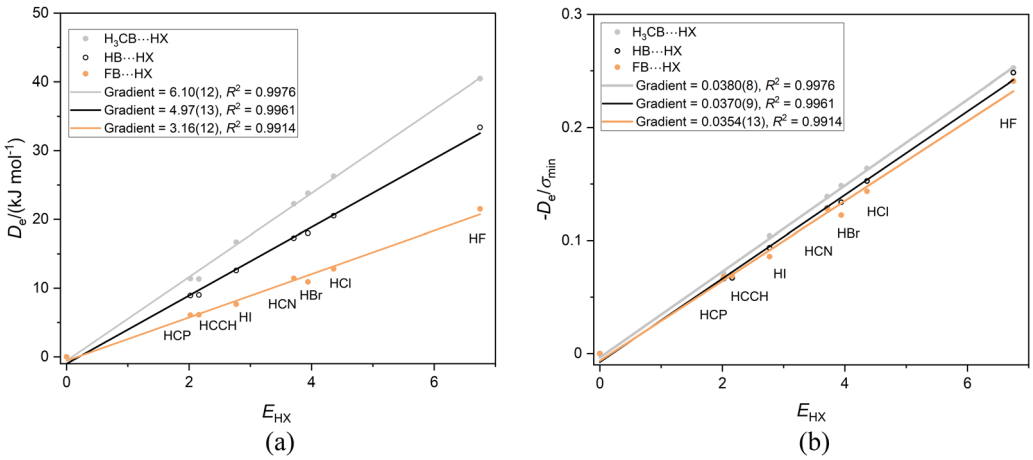

Fig. 6 (a) A plot of D_e *versus* E_{HX} for the series CH_3B···HX, HB···HX and FB···HX, (X = F, Cl, Br, I, C≡N. C≡CH and C≡P). (b) A plot of D_e/σ_{min} for the same three series.

Open Access Article. Published on 13 October 2022. Downloaded on 11/19/2024 11:00:08 PM.
This article is licensed under a Creative Commons Attribution 3.0 Unported Licence.

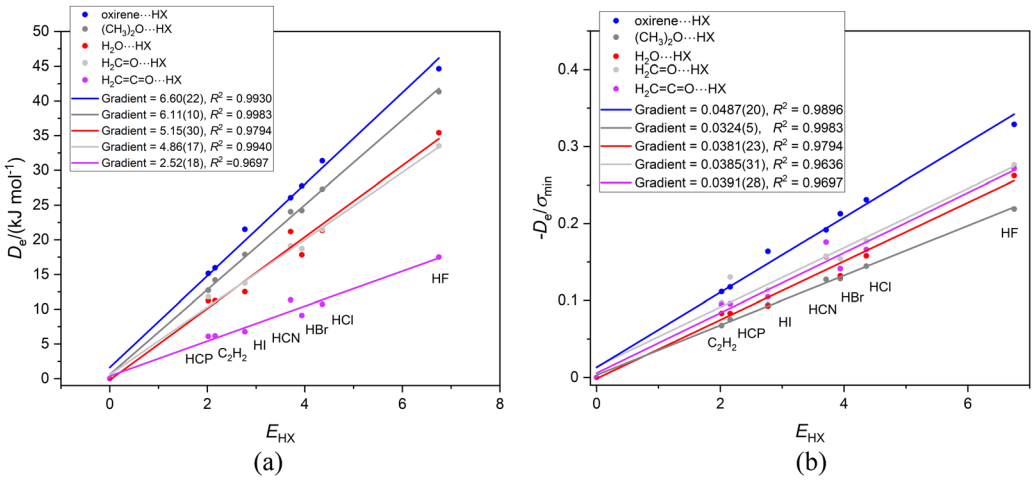

Fig. 7 (a) Graphs of D_e *versus* the electrophilicity E_{HX} of the hydrogen bond donor HX for five asymmetric-top Lewis bases B. The hydrogen bond is to the oxygen atom in each case and leads to a pyramidal configuration around this atom.

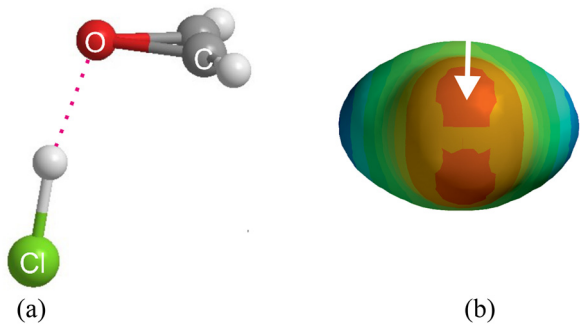

Fig. 8 (a) The CCSD(T)(F12c)/cc-pVDZ-F12 optimised geometry of oxirene···HCl drawn to scale. The angle between the H···O line and the oxirene C_2 axis is 64.6°. (b) The MESP of oxirene on the 0.001 e bohr^{-3} iso-surface calculated at the M06-2X/aug-cc-pVDZ level. The molecule is viewed from O along the C_2 axis, with the region of most negative potential energy (greatest nucleophilicity) corresponding to the axis of a non-bonding pair on O, as indicated by the arrow. The estimated angle made by the axis of the n-pair with the molecular C_2 axis is ∼60°.

Fig. 7(b) reveals that the gradients of the D_e/σ_{min} *versus* E_{HX} graphs for $H_2C{=}O$, $H_2C{=}C{=}O$ and H_2O are similar to those noted in Section 3.4 for O═C═O···HX and S═C═O···HX as the Lewis bases, namely ∼0.038, but that when $(CH_3)_2O$ is the Lewis base the value is slightly lower (0.032), while that for B = oxirene is much higher at 0.049. The reason for the behaviour when oxirene is the Lewis base is not clear, but we note that in Fig. 7(a) the intercept on the D_e axis for the B = oxirene line has the high value +1.6 kJ mol^{-1}.

We now examine the corresponding series of asymmetric-top molecules B in which S is the hydrogen-bond acceptor atom in place of O, namely dimethyl sulfide, $(CH_3)_2S$, thiirene (or thiacyclopropene), hydrogen sulfide, H_2S and thioformaldehyde, $H_2C{=}S$. In each case, the HX forms a hydrogen bond to S and makes an angle of close to 90° with the C_2 axis of B, as is known experimentally from a rotational spectroscopic investigation of the H_2S···HCl complex,[44] for example, and is confirmed by the results of the *ab initio* calculations conducted here (see ESI† for atomic coordinates). Fig. 9(a) shows the *ab initio* calculated geometry of thiirene···HCl. The angle H···S-* made by the hydrogen bond with the C_2 axis of thiirene is ∼90° (* is the centre of the C═C bond), The angle Cl–H···S is ∼ 170° and suggests a weak, secondary non-covalent interaction of Cl with the two electrophilic hydrogen atoms of thiirene. The molecular electrostatic surface potential (MESP) of thiirene calculated at the M06-2X/aug-cc-pVDZ level is displayed in Fig. 9(b). The front surface has been cut away to reveal the model of thiirene inside in a similar orientation to that shown in Fig. 9(a). The most nucleophilic (negative) region is coloured red and corresponds to the non-bonding electron pair direction below S at ∼90° to the molecular plane, as indicated by the arrow. The blue surfaces near to the two H atoms are the

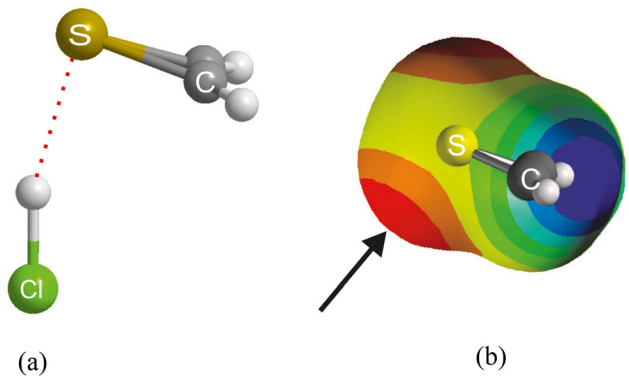

Fig. 9 (a) The geometry of thiirene···HCl, as calculated at the CCSD(T)(F12c)/cc-pVDZ-F12 level of theory. Note that the Cl atom is apparently involved in a (weak) secondary interaction with the two H atoms of thiirene. (b) Molecular electrostatic surface potential (MESP) of thiirene calculated at the M06-2X/aug-cc-pVDZ level on the 0.001 e bohr^{-3} iso-surface. The plane of the paper coincides with the symmetry plane of the molecule. The front surface of the MESP is cut away. The red regions of the MESP above and below S are the most nucleophilic regions of the molecule and correspond to the non-bonding electron pairs on S. The arrow indicates the axis of one of the non-bonding pairs, which make an angle of ∼90° with the heavy atom plane.

Open Access Article. Published on 13 October 2022. Downloaded on 11/19/2024 11:00:08 PM.
This article is licensed under a Creative Commons Attribution 3.0 Unported Licence.

most positive (electrophilic) regions of the thiirene molecule and are responsible for the weak secondary interaction involving Cl.

The graphs of D_e *versus* E_{HX} and D_e/σ_{min} *versus* E_{HX} for the group of complexes B···HX (X = F, Cl, Br, I, CN, CCH, CP) in which hydrogen bond is to the sulfur atom of the Lewis base B are in Fig. 10(a) and (b), respectively. In these diagrams, the origin was not fitted as a point because it is obvious that, when extrapolated, the calculated points for at least three of the series would not pass close to zero. Also included in Fig. 10 for interest is the graph for the series S_2···HX, in which S_2 is treated as a $^1\Sigma_g^+$ molecule (instead of the observed ground state $^3\Sigma_g^-$). It fits the pattern exhibited by the other B···HX complexes in the Fig. 10. One possible reason why some of the straight lines in Fig. 10(a) and (b) do not pass through the origin is that in these complexes there is larger dispersion contribution to D_e. The Lewis bases B contain the second row atom S and their complexes have a right-angled geometry (see Fig. 9(a)) which could also lead to an increased dispersion energy resulting from contiguity of X and B. It seems unlikely that division of D_e by the electrostatic quantity σ_{min} would allow for any dispersion contribution to D_e. Another possible factor is that the right-angled geometry gives more weight than in linear geometries to an interaction of electrophilic regions in B with the electrophilic atom in X (see Fig. 9(a) and (b)). Note that the gradients of the D_e/σ_{min} straight lines when the second row atom S is involved in the hydrogen bond are larger than found for the O analogues.

3.7 Symmetric-top complexes in which the hydrogen bond is to a pyramidal nitrogen or phosphorus atom

In this section, the complexes to be discussed are of the type R_3M···HX, in which M = N or P, R = Cl, H or CH_3, and X = F, Cl,

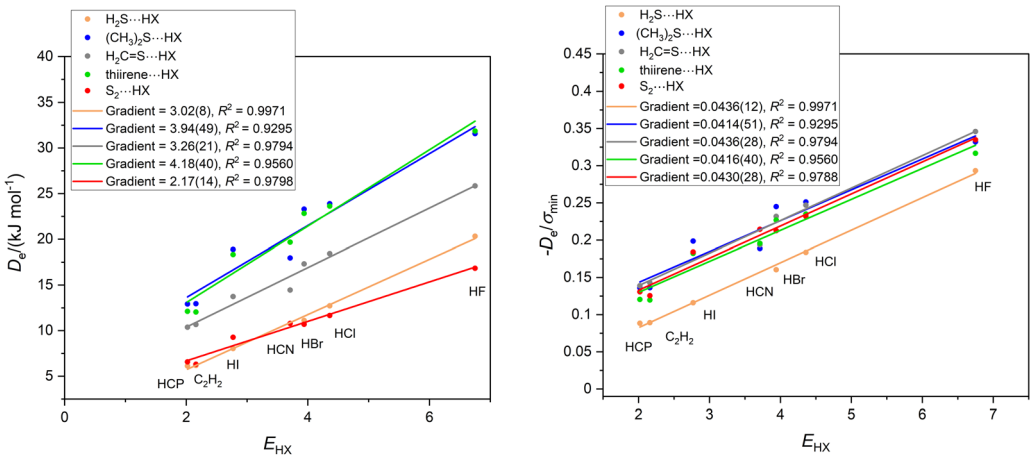

Fig. 10 (a) Graphs of D_e *versus* the electrophilicity E_{HX} of the hydrogen-bond donor HX for five Lewis bases B containing a sulfur atom. The hydrogen bond is to the sulfur atom and almost perpendicular to the local symmetry axis of B in each case. The origin is not included as a point in any line in this figure. (b) The corresponding graphs of D_e/σ_{min} *versus* E_{HX} for the complexes shown in (a). Note that the gradients in (b) are now identical within the errors of the fits, which is not so when the origin is included as a point.

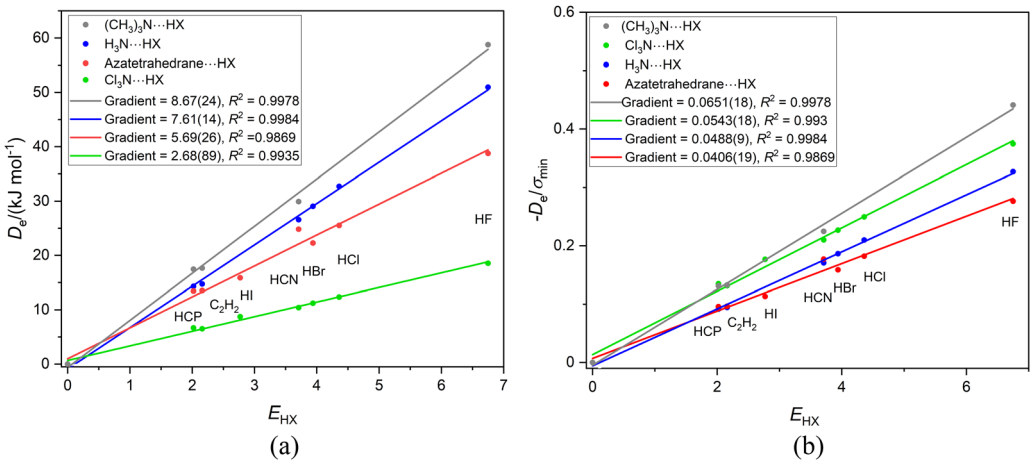

Fig. 11 Graphs of (a) D_e *versus* E_{HX} and (b) D_e/σ_{min} *versus* E_{HX} for the series of hydrogen-bonded complexes B···HX, where B = $(CH_3)_3N$, 1-azatetrahedrane, H_3N or Cl_3N and X = F, Cl, Br, I, CN, CCH and CP.

Open Access Article. Published on 13 October 2022. Downloaded on 11/19/2024 11:00:08 PM.
This article is licensed under a Creative Commons Attribution 3.0 Unported Licence.

Br, I, CN, CCH and CP. Calculations of $(CH_3)_3N\cdots HX$ for X = Cl, Br and I at the CCSD(T)(F12c)/cc-pVDZ-F12 level led to optimised geometries that were of the ion-pair type $(CH_3)_3NH^+\cdots X^-$ and points for these complexes were not included in the graph for the series. To compensate for this shortfall, the series in which another tertiary amine of C_{3v} symmetry, aza-tetrahedrane, is the Lewis base was also included. Fig. 11(a) is a plot of D_e *versus* E_{HX} for the four series $(CH_3)_3N\cdots HX$, 1-aza-tetrahedrane$\cdots$HX, $H_3N\cdots HX$ and $Cl_3N\cdots HX$, with X = F, Cl, Br, I, CN, CCH and CP as before. This set of nitrogen bases has groups attached to N that are electron-donating (CH_3) and electron-withdrawing (Cl) relative to H. The gradients of the straight lines in Fig. 11(a) yield the nucleophilicities of the Lewis bases and these are in the order $(CH_3)_3N\cdots HX > H_3N > Cl_3N$, as expected. The nucleophilicity of 1-aza-tetrahedrane is smaller than that of NH_3.

It is clear from Fig. 11(b) that, unlike other complexes involving N as the hydrogen-bond acceptor atom, such as $N_2\cdots HX$ and $PN\cdots HX$ (see Section 3.3 and Fig. 4), the division of D_e by σ_{min} does not yield a set of straight lines of the same gradient and consequently a reduced nucleophilicity $И_{R_3N}$ cannot be assigned to the pyramidal N atom in these species. Is there a reason for this?

Fig. 12 compares the MESPs of the four Lewis bases under discussion, all calculated at the M06-2X/aug-cc-VDZ level. Fig. 12(b) shows trimethylamine, in which the blue (electrophilic) regions associated with the H atoms are close to the central nucleophilic red region on the C_3 axis associated with the nitrogen n-pair, and they are also close to and surround the H atom of HX. For ammonia in Fig. 12(a) the blue electrophilic regions near to the H atoms are also quite close to the H atom of HX in the $H_3N\cdots HX$ complex by virtue of the very short N–H bonds. The geometry of 1-aza-tetrahedrane (shown in Fig. 12(c)) is such that the three H atoms are held well away from the pyramidal N atom and therefore these electrophilic (blue) regions are unlikely to have such a serious effect on the H atom of HX in the azatetrahedrane$\cdots$HX complex. NCl_3 (Fig. 12(d)) has off-axis (orange-red) nucleophilic regions associated with the Cl atoms that presumably reinforce the effect of the axial nucleophilic region associated with the N atom. Thus, it seems that the value of the reduced nucleophilicity $И_{R_3N}$ for pyramidal N in symmetric-top molecules (*i.e.* the gradient of the D_e/σ_{min} *versus* E_{HX} plot) most likely to be correct is 0.0406(19) determined for the aza-tetrahedrane complex. This value is similar within the error of the linear regression fits to (but not quite identical with) those

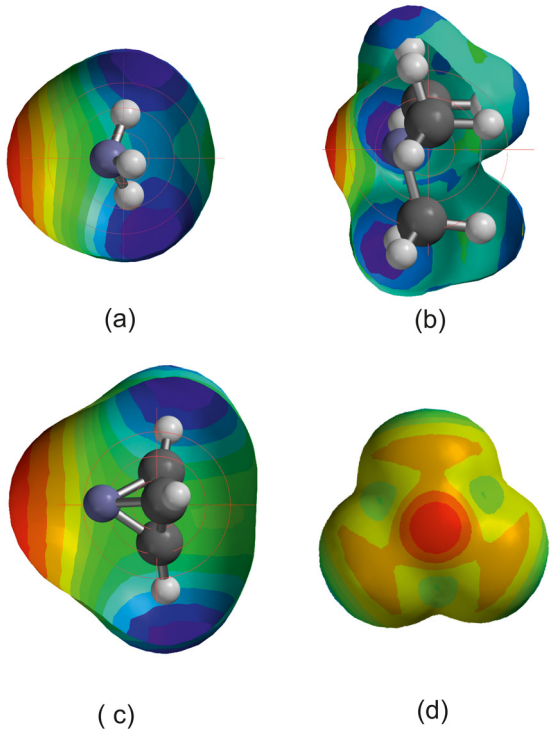

Fig. 12 Molecular electrostatic surface potentials of the symmetric-top molecules (a) ammonia, (b) trimethylamine, (c) 1-azatetrahedrane and (d) trichloramine. Some of the surface has been cut away to reveal the ball and spoke models of the molecules within for (a)–(c). The view is perpendicular to the C_3 axis in these cases while in (d) the view is along this axis with the N atom nearer to the viewer than the Cl atoms, and no surface is cut away.

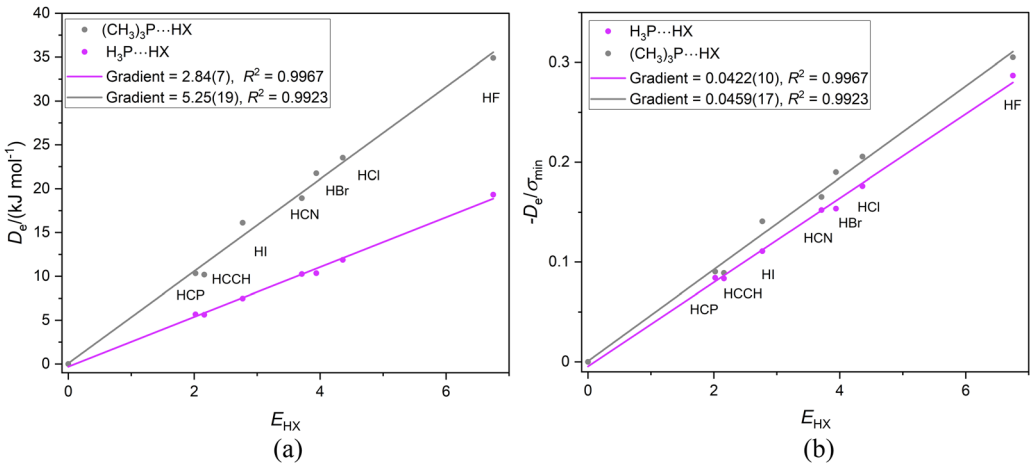

Fig. 13 (a) D_e *versus* E_{HX} and (b) D_e/σ_{min} *versus* E_{HX} for the two series of complexes $H_3P\cdots HX$ and $(CH_3)_3P\cdots HX$ (X = F, Cl, Br, I, CN, CCH, CP).

Open Access Article. Published on 13 October 2022. Downloaded on 11/19/2024 11:00:08 PM.
This article is licensed under a Creative Commons Attribution 3.0 Unported Licence.

determined [mean 0.0375(10)] for the linear complexes $N_2\cdots HX$ and $PN\cdots HX$ involving N as the H-bond acceptor.

If the proximity of the electrophilic H atoms of ammonia or trimethylamine to the H atom of HX in complexes $H_3N\cdots HX$ and $(CH_3)_3N\cdots HX$ causes problems with obtaining a reduced nucleophilicity $И_{R_3N}$ for ammonia and trimethylamine, it is possible that substitution of N by a P atom and the consequent greater H–P and C–P distances in H_3P and $(CH_3)_3P$, respectively, will remove this impediment. Fig. 13(a) shows the D_e *versus* E_{HX} points for the $H_3P\cdots HX$ and $(CH_3)_3P\cdots HX$ series of complexes. As expected from the +I effect of CH_3 relative to H, the gradient of the linear regression fit to the points for the trimethylphosphine complexes (and hence the nucleophilicity) is greater than that for the phosphine complexes. Fig. 13(b) demonstrates that division of D_e values by the minimum value of the MESP (which occurs on the C_3 axis just outside the P atom and is a property of the non-bonding electron pair of P) causes the two straight-line fits to have essentially equal gradients and suggests a reduced nucleophilicity of $И_{R_3P}$ = 0.0441(17) for the $(CH_3)_3P$ and H_3P Lewis bases. Interestingly, the mean value for five complexes $B\cdots HX$ in which the hydrogen bond is to an S atom of B is 0.0426(10). See Section 3.6 and Fig. 10(b).

4. Conclusions

In this article, we have used *ab initio* calculations at the CCSD(T)(F12c)/cc-pVDZ-F12 level to determine the equilibrium dissociation energies D_e of a large number ($\sim$190) of hydrogen-bonded complexes of the type $B\cdots HX$, where B is a simple Lewis base molecule and X = F, Cl, Br, I, CN, CCH, CP. Plots of D_e *versus* E_{HX}, where E_{HX} is the electrophilicity[32] of the molecule HX, are in most cases reasonably good straight lines through the origin. The gradient of each straight line gives a measure of the nucleophilicity N_B of the Lewis base B, as discussed in the Introduction in connection with eqn (1)–(4). This definition of the nucleophilicity of B applies to the weak interaction of B with the series of Lewis acids HX in isolation in the gas phase. As pointed out in an earlier publication[42] the values of N_B can, in suitable cases, be used to define a numerical scale of the inductive effect of groups attached to the atom directly involved in the $B\cdots HX$ hydrogen bond. For example, in this work, the relative inductive effects of CH_3 groups and halogen atoms have been compared.

The main aim of the investigations reported here was to find whether it is possible to define a reduced nucleophilicity of Lewis base molecules B having a common terminal atom (*e.g.* N in HCN FCN and CH_3CN as discussed in (Section 3.3)) when forming hydrogen bonds to a series of Lewis acids HX. The focus here has been on the particular series in which X = F, Cl, Br, I, CN, CCH and CP. In an analogous approach, reported earlier,[32] dissociation energies D_e of complexes formed by a fixed Lewis acid (*e.g.* HF) with a series of several different Lewis bases B were plotted against the nucleophilicities N_B of the Lewis bases. The resulting straight line through the origin yielded the electrophilicity E_{HX} of the Lewis acid HX. It was discovered that when D_e was divided by σ_{max}, the maximum value of the molecular electrostatic surface potential of the Lewis acid (and therefore its most electrophilic region for interactions that are mainly electrostatic in character), the graphs of D_e/σ_{max} against N_B for several different Lewis acids (*e.g.* HF, HCl, HBr, HI) degenerated to a single straight line. The gradient of this line provided a reduced electrophilicity Ξ_{HX} that is a property of the electrophilic end H of HX and is independent of X. σ_{min} is the quantity for a Lewis base that corresponds to σ_{max} of a Lewis acid and is the minimum value of the MESP. It is often associated with the direction of the axis of a non-bonding electron pair of B. We have here asked the following question: does a plot of D_e/σ_{min} against the E_{HX} (*i.e.* the electrophilicities of a series of Lewis acids HX) lead (as previewed in eqn (4) in the Introduction) to a single straight line of gradient $И_B$ for molecules B having a common terminal atom directly involved in the hydrogen bond from HX to B?

The answer to this question is evident from the graphs displayed in Fig. 1–7, 10, 11 and 13. The gradients of the D_e/σ_{min} *versus* E_{HX} plots have been abstracted from the various figures and are displayed in Table 3 in categories defined by the terminal atom involved in the hydrogen bond in various $B\cdots HX$

Table 3 Reduced nucleophilicities И determined for some first and second row atoms

Molecular type	H-bond acceptor atom	Complex	Reduced nucleophilicity, И[a]	Mean value of И[b]
Linear/sym. top	Boron	$H_3CB\cdots HX$	0.0380(8)	0.0368(10)
		$HB\cdots HX$	0.0370(9)	
		$FB\cdots HX$	0.0354(13)	
Linear	Carbon	$OC\cdots HX$	0.0346(26)	0.0349(17)
		$SC\cdots HX$	0.0355(15)	
		$SeC\cdots HX$	0.0345(11)	
Linear/sym. top	Carbon	$CH_3NC\cdots HX$	0.0343(16)	0.0337(18)
		$HNC\cdots HX$	0.0337(18)	
		$FNC\cdots HX$	0.0332(19)	
Linear/sym. top	Nitrogen	$CH_3CN\cdots HX$	0.0337(23)	0.0333(23)
		$HCN\cdots HX$	0.0329(24)	
		$FCN\cdots HX$	0.0333(23)	
Linear	Nitrogen	$PN\cdots HX$	0.0386(21)	0.0374(25)
		$N_2\cdots HX$	0.0363(30)	
Linear	Oxygen	$OCO\cdots HX$	0.0372(36)	0.0376(36)
		$SCO\cdots HX$	0.0380(37)	
Asym. top	Oxygen	$H_2O\cdots HX$	0.0381(23)	0.0386(27)
		$H_2CO\cdots HX$	0.0385(31)	
		$H_2CCO\cdots HX$	0.0391(28)	
Asym. top	Sulfur	$H_2S\cdots HX$	0.0436(12)	0.0427(33)
		$(CH_3)_2S\cdots HX$	0.0414(51)	
		$H_2CS\cdots HX$	0.0436(28)	
		Thiirene$\cdots HX$	0.0416(40)	
		$S_2\cdots HX$	0.0430(28)	
Sym. top	Phosphorus	$H_3P\cdots HX$	0.0459(17)	0.0441(14)
		$(CH_3)_3P\cdots HX$	0.0422(10)	

[a] И is the gradient of the linear regression fit to the points of the D_e/σ_{min} *versus* E_{HX} graph in each case (see Fig. 1–7 and 10–13). HX is Lewis acid H-bond donor, with X = F, Cl, Br, I, CN, CCH, CP. $И_B$ is defined as the reduced nucleophilicity of the Lewis base B. [b] The mean value of $И_B$ for the indicated group of complexes. The error given is the mean of the errors generated in the linear regression fit of each of the relevant D_e/σ_{min} *versus* E_{HX} plots.

Open Access Article. Published on 13 October 2022. Downloaded on 11/19/2024 11:00:08 PM.
This article is licensed under a Creative Commons Attribution 3.0 Unported Licence.

complexes. The order of the categories is the order of the terminal atoms in the Periodic Table. The conclusion is clear, namely that the gradients of the linear regression fits to points for a given category of Lewis base B are identical or nearly so (within the error of the fit) when the molecules B are different but when the same atom is directly involved in the hydrogen bonds to HX. This seems to be established, even though the errors associated with the fits are larger than desirable in some cases. The exception to this conclusion is the series in which the Lewis bases are asymmetric-top molecules carrying an oxygen atom, the results for which are not included in Table 3. Some possible reasons for the exceptional behaviour have been tentatively presented. In Table 3, the final column carries the mean of the values (and the quoted error is the mean of the error of the various fits) in each separate category. The following striking conclusion is available from Table 3: not only is the reduced nucleophilicity $И_B$ independent of the remainder of the molecule B attached to the atom involved in the hydrogen bond with HX, but also there is evidence that the quantity is very similar for all the first row atoms and that these appear to be smaller than those of the second row atoms investigated, that is S and P. It seems reasonable that second row atoms should have a larger nucleophilicity that their first row counterparts in view of their greater numbers of electrons. Thus, we have established the existence of the reduced nucleophilicity $И_B$ of Lewis bases B to match the earlier conclusion[32] that there exists a reduced electrophilicity Ξ_A of Lewis acids A.

Conflicts of interest

There are no conflicts of interest to declare.

Acknowledgements

A. C. L. thanks the University of Bristol for the award of a University Senior Research Fellowship. I. A. thanks the Ministerio de Ciencia e Innovación of Spain (PGC2018-094644-B-C22 and PID2021-125207NB-C32) and Comunidad de Madrid (P2018/EMT-4329 AIRTEC-CM) for financial support.

References

1 R. S. Drago and B. B. Wayland, *J. Am. Chem. Soc.*, 1965, **87**, 3571–3577.
2 M. K. Kroeger and R. S. Drago, *J. Am. Chem. Soc.*, 1981, **103**, 3250–3262.
3 D. Gurka and R. W. Taft, *J. Am. Chem. Soc.*, 1969, **91**, 4794–4801.
4 M. R. Abraham, P. P. Duce, P. L. Grellier, D. V. Prior, J. J. Morris and P. J. Taylor, *Tetrahedron Lett.*, 1988, **29**, 1587–1590.
5 M. H. Abraham, P. L. Grellier, D. V. Prior, R. W. Taft, J. J. Morris, P. J. Taylor, C. Laurence, M. Berthelot and R. M. Doherty, *et al.*, *J. Am. Chem. Soc.*, 1988, **110**, 8534–8536.
6 M. H. Abraham, *Chem. Soc. Rev.*, 1993, **22**, 73–83.
7 J. Marco, J. M. Orza, R. Notario and J.-L. M. Abboud, *J. Am. Chem. Soc.*, 1994, **116**, 8841–8842.
8 J. A. Platts, *Phys. Chem. Chem. Phys.*, 2000, **2**, 973–980.
9 J. A. Platts, *Phys. Chem. Chem. Phys.*, 2000, **2**, 3115–3120.
10 O. Lamarche and J. A. Platts, *Chem. – Eur. J.*, 2002, **8**, 457–466.
11 O. Lamarche and J. A. Platts, *Phys. Chem. Chem. Phys.*, 2003, **5**, 677–684.
12 T. Steiner and W. Saenger, *Acta Crystallogr., Sect. B: Struct. Sci.*, 1994, **50**, 348–357.
13 T. Steiner, *J. Chem. Soc., Chem. Commun.*, 1995, 1331–1332.
14 T. Steiner, *J. Phys. Chem. A*, 1998, **102**, 7041–7052.
15 H. Benedict, H.-H. Limbach, M. Wehlan, W.-P. Fehlhammer, N. S. Golubev and R. Janoschek, *J. Am. Chem. Soc.*, 1998, **120**, 2939–2950.
16 H. Benedict, I. G. Shenderovich, O. L. Malkina, V. G. Malkin, G. S. Denisov, N. S. Golubev and H.-H. Limbach, *J. Am. Chem. Soc.*, 2000, **122**, 1979–1988.
17 I. Alkorta and J. Elguero, *Struct. Chem.*, 1999, **10**, 157–159.
18 M. Ramos, I. Alkorta, J. Elguero, N. S. Golubev, G. S. Denisov, H. Benedict and H.-H. Limbach, *J. Phys. Chem. A*, 1997, **101**, 9791–9800.
19 E. Espinosa, I. Alkorta, J. Elguero and E. Molins, *J. Chem. Phys.*, 2002, **117**, 5529–5542.
20 I. Alkorta, I. Rozas and J. Elguero, *Struct. Chem.*, 1998, **9**, 243–247.
21 C. K. Ingold, *J. Chem. Soc.*, 1933, 1120–1127.
22 H. Mayr and M. Patz, *Angew. Chem., Int. Ed. Engl.*, 1994, **33**, 938–957.
23 H. Mayr, *Angew. Chem., Int. Ed.*, 2011, **50**, 3612–3618.
24 A. C. Legon and D. J. Millen, *J. Am. Chem. Soc.*, 1987, **109**, 356–358.
25 A. C. Legon, *Phys. Chem. Chem. Phys.*, 2014, **16**, 12415–12421 and corrected, 2014, **16**, 25199.
26 I. Alkorta and A. C. Legon, *New J. Chem.*, 2018, **42**, 10548–10554.
27 I. Alkorta and A. C. Legon, *Molecules*, 2017, **22**, 1786–1799.
28 I. Alkorta, N. R. Walker and A. C. Legon, *Inorganics*, 2021, **9**, 13.
29 I. Alkorta, J. G. Hill and A. C. Legon, *Phys. Chem. Chem. Phys.*, 2020, **22**, 16421–16430.
30 A. D. Buckingham and P. W. Fowler, *Can. J. Chem.*, 1985, **63**, 2018–2025.
31 J. S. Murray and P. Politzer, *Wiley Interdiscip. Rev.: Comput. Mol. Sci.*, 2017, **7**, 326.
32 I. Alkorta and A. C. Legon, *Phys. Chem. Chem. Phys.*, 2022, **24**, 6856–6865.
33 *Dimensionless Physical Quantities in Science and Engineering*, ed. J. Kuneš, Elsevier, Amsterdam, 1st Edn, 2010.
34 C. Hättig, D. P. Tew and A. Köhn, *J. Chem. Phys.*, 2010, **132**, 231102.
35 C. Hättig, W. Klopper, A. Köhn and D. P. Tew, *Chem. Rev.*, 2012, **112**, 4–74.
36 J. G. Hill and K. A. Peterson, *J. Chem. Phys.*, 2014, **141**, 094106.

 This journal is © the Owner Societies 2022

Open Access Article. Published on 13 October 2022. Downloaded on 11/19/2024 11:00:08 PM.
This article is licensed under a Creative Commons Attribution 3.0 Unported Licence.

37 S. F. Boys and F. Bernardi, *Mol. Phys.*, 1970, **19**, 553–566.
38 H.-J. Werner, P. J. Knowles, G. Knizia, F. R. Manby and M. Schütz, *Wiley Interdiscip. Rev.: Comput. Mol. Sci.*, 2012, **2**, 242–253.
39 M. J. Frisch, G. W. Trucks, H. B. Schlegel, G. E. Scuseria, M. A. Robb, J. R. Cheeseman, G. Scalmani, V. Barone, G. A. Petersson and H. Nakatsuji, *et al.*, *Gaussian 16; Revision, A.03*, Gaussian, Inc., Wallingford, CT, USA, 2016.
40 T. Lu and F. Chen, *J. Comput. Chem.*, 2012, **33**, 580–592.
41 Spartan 20; Wavefunction, Inc.: Irvine, CA, 2020. Spartan is an interface running the Q-Chem engine underneath. Except for molecular mechanics and semi-empirical models, the calculation methods used by Spartan are those of Q-Chem and are documented in: Y. Shao, L. F. Molnar, Y. Jung, J. Kussmann, C. Ochsenfeld, S. T. Brown, A. T. B. Gilbert, L. V. Slipchenko, S. V. Levchenko, D. P. O'Neill, R. A. DiStasio Jr., R. C. Lochan, T. Wang, G. J. O. Beran, N. A. Besley, J. M. Herbert, C. Y. Lin, T. Van Voorhis, S. H. Chien, A. Sodt, R. P. Steele, V. A. Rassolov, P. E. Maslen, P. P. Korambath, R. D. Adamson, B. Austin, J. Baker, E. F. C. Byrd, H. Dachsel, R. J. Doerksen, A. Dreuw, B. D. Dunietz, A. D. Dutoi, T. R. Furlani, S. R. Gwaltney, A. Heyden, S. Hirata, C.-P. Hsu, G. Kedziora, R. Z. Khalliulin, P. Klunzinger, A. M. Lee, M. S. Lee, W. Z. Liang, I. Lotan, N. Nair, B. Peters, E. I. Proynov, P. A. Pieniazek, Y. M. Rhee, J. Ritchie, E. Rosta, C. D. Sherrill, A. C. Simmonett, J. E. Subotnik, H. L. Woodcock III, W. Zhang, A. T. Bell, A. K. Chakraborty, D. M. Chipman, F. J. Keil, A. Warshel, W. J. Hehre, H. F. Schaefer, J. Kong, A. I. Krylov, P. M. W. Gill and M. Head-Gordon, *Phys. Chem. Chem. Phys.*, 2006, **8**, 3172.
42 I. Alkorta and A. C. Legon, *Phys. Chem. Chem. Phys.*, 2022, **24**, 12804–12807.
43 Z. Kisiel, B. A. Pietrewicz, P. W. Fowler, A. C. Legon and E. Steiner, *J. Phys. Chem.*, 2000, **104**, 6970–6978.
44 E. J. Goodwin and A. C. Legon, *J. Chem. Soc., Faraday Trans. 2*, 1984, **80**, 51–65.